Chapter 10

Contribution of electric vehicles to power system ancillary services beyond distributed energy storage

Sergio Martinez[1], Hugo Mendonça[1], Rosa M. de Castro[1] and Danny Ochoa[1]

Current electric power systems are experiencing a steady growth in renewable electricity generation and in energy consumption from electric vehicles (EV), involving a number of impacts on the system that increase with the penetration level and the system weakness. As conventional synchronous generation is being displaced by renewable generators, they must take their share in the ancillary services provision and supplementary equipment has to be installed, with its associated cost. This chapter describes how EVs, already connected to the grid with appropriate electronic converters and controls, can be used for contributing to the provision of frequency and voltage control, thus avoiding additional investment in supplementary equipment. The chapter also presents innovative approaches for both ancillary services, based on previous developments in electricity generation from wind and wave energies.

List of abbreviations

AC	Alternating Current
BESS	Battery Energy Storage System
DC	Direct Current
DG	Distributed Generation
EV	Electric Vehicle
LFC	Load Frequency Control
LV	Low Voltage
PQ	Active power and reactive power specified
PV	Active power and voltage specified

[1]Department of Electrical Engineering, ETSI Industriales, Universidad Politecnica de Madrid, Madrid, Spain

rms	Root Mean Square
RoCoF	Rate of Change of Frequency
SAVFI	System Average Voltage Fluctuation Index
SoC	State of Charge

10.1 Introduction

Current electric power systems have experienced an extraordinary growth in electricity generation from clean energy sources during the last years, mainly due to steady cost decline for wind and photovoltaic (PV) technologies [1]. This growth is expected to continue in the coming years along with an increase in the number of electric vehicles (EV) connected to the power system for recharging. Both renewable electricity generation and energy consumption from EVs involve a number of impacts on the power system to which they are connected, which increase with the penetration level and the system weakness [2]. Since this level is already high in the case of renewable generation and it will be steadily increasing in the case of EVs, power systems face the challenge to integrate them in a way so that reliability and efficiency are not affected [3].

To contribute to achieve this goal, a natural approach is to take advantage of the rising number of EVs connected to the grid, with an increasing storage capacity in their batteries, by using them as distributed energy storage for wind or PV plants [4]. Beyond this approach, apart from generating electricity, renewable generators should also be involved in providing ancillary services, such as voltage control, power-frequency control and other grid-support tasks. In older power systems, the bulk electrical energy was generated at conventional power plants, such as hydroelectric or thermal ones, equipped with synchronous electrical generators that, in addition to generating electricity, provided most of the ancillary services. In current power systems, the synchronous generation is being largely displaced by renewable generators, and they must also take their share in the ancillary services provision. As they do not have the same capabilities as the conventional plants they displace, supplementary equipment has to be installed, with its associated cost. EVs seem to be one of the eminent resources for providing various ancillary services due to their defining properties: they are a large load compared with other residential loads, they have quick response with potential bidirectional power flow capabilities and they are available most of the times with a high degree of flexibility [5]. This chapter describes how EVs with appropriate electronic converters and controls, which are already connected to the grid, can be used for contributing to the provision of frequency and voltage control thus avoiding additional investment in supplementary equipment. For example, [6] describes a field-test demonstration in a real Danish distribution grid with an EV providing three ancillary services through unidirectional AC charging.

In relation to the role of EVs in the frequency control of power systems with high levels of renewable generation, it is relevant that the intermittent and non-dispatchable character of wind and PV energy impacts the power system

performance in terms of frequency perturbations. Contribution of EVs to secondary and even tertiary frequency controls has been widely described in the literature, for example in [7] and [8]. Lately, some works that deal with taking advantage of EVs connected to the grid for primary power-frequency control have been published. For example, [9] presents a fuzzy controller that, in addition to secondary control, implements a primary frequency control based on perfect and non-delayed information. Section 10.2 of this chapter describes how EVs can contribute to primary power-frequency control and system inertia, and it also presents the authors' proposal for a decentralized control approach, independent of communication links, as an adaptation to connected EVs of the strategy presented in [10] for variable speed-wind turbines.

On the other hand, the reactive power support from distributed generation (DG) opens a range of possibilities to improve the voltage quality. Many approaches address the Volt/var control for voltage regulation, for example [11,12]. In this sense, EVs can be seen as a potential solution to contribute to the voltage regulation of highly renewable energy–penetrated power systems. In fact, [13] proposes a strategy to mitigate over/undervoltage issues by the interaction between electrical vehicles and on load tap-changing transformers. However, the DG penetration does not only affect the voltage level of the grid but also introduces voltage fluctuations caused by the nature of primary sources (solar, wind...) [14] formulates a set of rules that seem interesting to assess the voltage fluctuation in customers that share a distribution service transformer. Although they have been carried out only with PV generation, they could be extrapolated to any other DG. [15] summarizes the impact on the grid of fluctuating power generation and presents a fluctuation power index to relate the voltage fluctuation mitigation with the power fluctuation in the case of storage devices. Reference [16] also uses a storage device to smooth the voltage fluctuation. In this case, the DC-link charges and discharges to smooth the voltage fluctuation in the AC-side. Other mitigating methods can be found in [17] and references therein. Section 10.3 describes how a fluctuating active power injection leads to grid voltage fluctuations and presents the authors' proposal of a reactive power controller for mitigating those fluctuations by using EVs already connected for recharging, without any other additional equipment. This proposal is a simple yet effective adaptation of a control strategy previously developed by the authors for wave energy–conversion systems [18].

10.2 Contribution of electric vehicles to the power system frequency control

As stated in the introduction, this section of the chapter aims at describing how secondary and tertiary frequency controls can be complemented in the short and very short terms with the contribution of EVs to primary power-frequency control and system inertia. The section describes the theoretical basis of the problem and how EVs connected to the grid for recharging can be used for mitigating frequency perturbations by means of an intelligent control on their charging process.

The phenomena involved and the performance of the proposed strategy are illustrated with simulations on a test network.

10.2.1 Theoretical background

In general, the frequency of a power system has to be kept constant, but it depends on the active power balance in the system. A variation of the active power consumed by a load at a given bus leads to a frequency variation in the whole system, reproduced as a speed variation in synchronous rotating generators. As frequencies or speed variations are the consequence of active power imbalance in the system, they are used as control signals for its compensation by acting on the active power injected by generators. Primary (fastest) frequency control is performed by the speed governors of generators and secondary and tertiary (slowest) controls are used for allocating generation.

10.2.2 Case study

In order to illustrate the potential contribution of the EV to the grid-frequency-control tasks when it is plugged into the network, the simple power system depicted in Figure 10.1 will be considered as a case of study. This power system is characterized by two conventional generation technologies: hydroelectric and thermal, which are supplying a single electric load. On the demand side, the aggregated effect of the integration of EVs under recharging has also been considered. According to this approach, the EV is seen as a battery energy storage system (BESS) from the grid side. This BESS is equipped with a grid-connection interface based on a power electronic converter. In this diagram, P_{BESS} is the three-phase active power injected or consumed by the EV-Battery under discharge and charge conditions, respectively. The selection of one or another operation mode will depend on certain control criteria implemented in the power controller that governs the DC/AC converter; although, it is important to mention that, traditionally, the EV is considered as an energy-consumption component of the grid.

Figure 10.2 illustrates the load frequency control (LFC) scheme that represents the short-term dynamics of the power system under study [19]. This representation

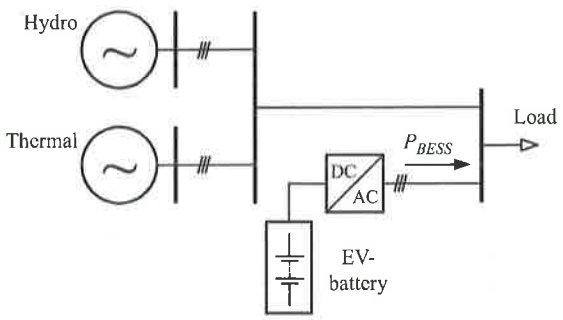

Figure 10.1 Test power system

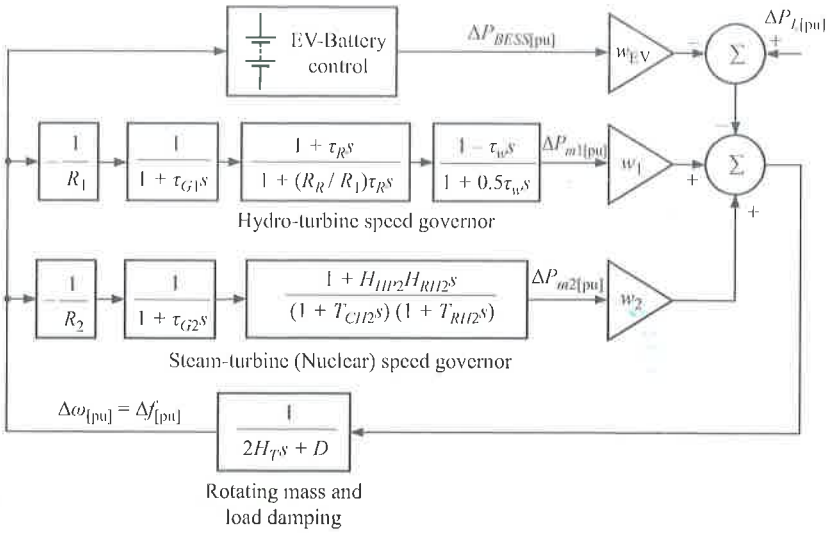

Figure 10.2 LFC scheme of the test power system

Table 10.1 Constant of inertia and LFC-participation weights of the generation technologies

Type of power plant	H_i**(s)**	w_i **(%)**
Hydro	3.6	40
Thermal (Nuclear)	7	40
EV-Battery	–	20

is derived from the swing equation of a synchronous generator, linearized by considering small deviations of the variables involved. In this scheme, the constant of inertia, H_T, represents all the available inertial resources and it is constituted by the individual constant of inertia of the operating synchronous generation groups, whose typical values are listed in Table 10.1 [19,20].

On the other hand, the time frame used in this type of analysis (usually, in the order of the seconds) allows focusing the study of the temporal behaviour of conventional generation technologies on the response of the speed governors of their respective mechanical drives. The simplified models of the speed governors that are shown in Figure 10.2 are taken from [19], and the typical values of their variables are summarized in Table 10.2.

ΔP_{m1} and ΔP_{m2} are the deviations of the mechanical power of the mechanical drives of the hydraulic and thermal generator in response to the presence of grid-frequency deviations, $\Delta\omega$. ΔP_L is the electric load deviation and, for this case of study, the only source of disturbance. The damping effect of the load is represented by the constant D (where a typical value of 0.5 p.u. has been taken for this

Table 10.2 Speed governor parameters

Parameter	Value and units	
	Hydro	**Thermal**
Droop, R	5%	5%
Main servo time constant, τ_G	0.2 s	0.2 s
Maximum gate opening rate	0.16 pu/s	0.05 pu/s
Maximum gate closing rate	– 0.16 pu/s	– 0.1 pu/s
Water time constant, τ_W	1 s	
Temporary droop, R_T	0.4 pu	
Reset time, τ_R	5 s	
Fraction of total turbine power generated by high pressure, F_{HP}		0.3
Reheater time constant, T_{RH}		5 s
Time constant of main inlet columns and steam chest, T_{CH}		0.3 s

example). ΔP_{BESS} is the injected/consumed EV-Battery active power deviation. Within the considered time scale, this variable will be practically negligible due to the slow charging and discharging process. However, when a grid-frequency-sensitive algorithm is implemented on the active power controller of the EV-Battery, the value of ΔP_{BESS} will begin to gain importance. All the variable deviations introduced before are defined regarding to their respective pre-disturbance values.

Finally, the terms w_1, w_2 and w_{EV} are the participation weights of each generation technology within the LFC scheme, which are defined as the ratio of their respective installed capacity and base power. In this case, the chosen base power corresponds to the total active power of the load. According to this criterion, these factors will reflect the energy share of each type of generation for the electrical load supplying. The assigned values for the participation weights are presented in Table 10.1.

The perturbation applied to the test power system is modelled as a sudden increase of 1% of the electric load. Therefore, it is expected that the frequency control tasks are carried out only by the synchronous generators by default. The time domain simulation results for this case of study are shown in Figure 10.3 as the grey solid lines. These illustrations that show the behaviour of the variables of interest: P_{BESS}, grid-frequency, and the rate of change of frequency (RoCoF), demonstrate that the EV-Battery charger does not contribute to reduce the grid frequency drop under normal operating mode.

However, if an adequate supplementary control scheme is implemented in the active power control of the EV-Battery charger, it is possible to provide this device with an emulated inertial response. The scheme used for this purpose is depicted in Figure 10.4, as an adaptation of the one proposed by [10]. This scheme has been originally devised to be implemented in a variable speed-wind turbine. Hence, after some modifications that scheme could be adapted for allowing its incorporation in the EV-Battery charger used in this study.

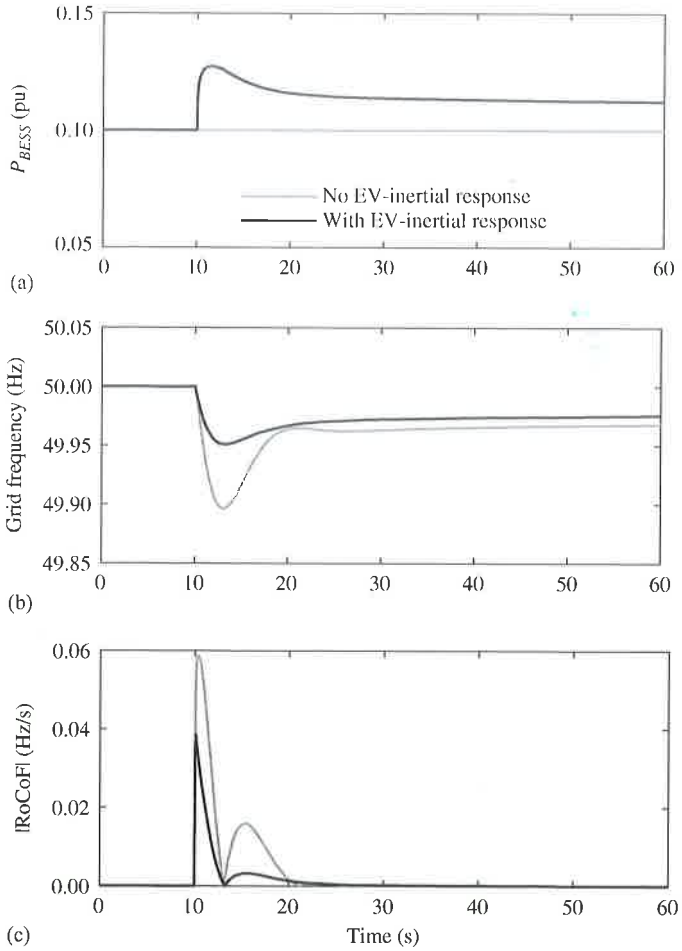

Figure 10.3 Time-domain simulation results: (a) Default EV-Battery charger operation mode (grey solid lines), (b) and (c) Frequency support provided by the EV-Battery charger (black solid lines)

The proposed frequency-control scheme has two control loops: one depends on the grid-frequency deviation (computed as the difference between the nominal frequency, f_{nom}, and the measured frequency, f_s) and the other one depends on the time derivative of the grid frequency. The output signals of both loops (ΔP_1^* and ΔP_2^*) are added to the default active power set-point of the battery charger, P_C^*. These three signals constitute the active power set-point signal of the modified EV-Battery charger, P_{BESS}^*. The dynamic gains that govern the control actions in the supplementary control scheme are defined by (10.1) and (10.2), and depend on the current state of charge (SoC) of the battery. In this example, the initial SoC is chosen as 0.5 p.u., the maximum state of charge (SoC_{max}) as 1 p.u., the initial droop

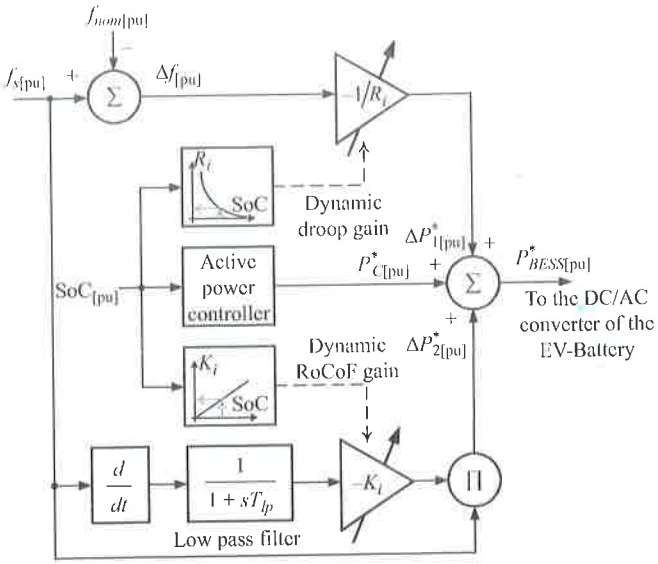

Figure 10.4 Frequency-control scheme implemented in the EV-Battery charger

(R_0) as 2%, the initial RoCoF-constant (K_0) as 50, and the time constant of the low-pass filter, T_{lp}, is set to 100 ms.

$$R_i = R_0\, SoC_{max\ [pu]}/SoC_{[pu]} \tag{10.1}$$

$$K_i = K_0\, SoC_{[pu]} \tag{10.2}$$

Black solid line plots in Figure 10.3 show the benefits of enabling the EV-Battery chargers to provide frequency support to the grid. For this example, the frequency nadir is reduced to 53% and the peak absolute rate of change of frequency is decreased to about 35%.

At this point, the reader should bear in mind that this simple example is intended to demonstrate that power systems can take advantage of the massive integration of EV into the grid for the provision of ancillary services, in this case, the frequency control. However, putting this into practice could constitute a challenging task from a technical, social and economic points of views due to several reasons, such as: the majority existence of single-phase charging stations with the consequent unbalance of the grid, the lack of policies that guarantee the availability of enough number of connected EVs for the provision of ancillary services, control strategies that allow guaranteeing an adequate level of charge when the EV is unplugged, the absence of economic policies for compensating the EV-owner since its battery is used for activities that are responsibility of the system operator, a conclusive research about the effects of the charge and discharge actions on the battery aging, and others.

10.3 Contribution of electric vehicles to voltage control

The fluctuation of the power injected into the grid by wind and PV generators impacts mainly on the power system frequency, and has an impact on the grid voltage. This section of the chapter describes how a fluctuating active power injection leads to grid voltage fluctuations and presents an unbalanced three-phase power flow algorithm that allows to quantitatively analyse the voltage evolution at every phase and bus of a distribution grid driven by this power injection. It also shows how connected EVs can be used for mitigating the grid voltage fluctuations by making use of the reactive capability of the grid-side converter. The performance of the strategy is illustrated with simulations on a test-distribution network based on the European low-voltage (LV) distribution network benchmark with DG from Cigré [21], which presents structural unbalance and unbalanced loads.

10.3.1 Theoretical background

To show how a fluctuating active power injection at a given bus leads to grid voltage fluctuations, let us consider a simplified representation (Figure 10.5) of the grid supplying the bus as a balanced system described by its Thévenin equivalent circuit, with voltage phasor $\underline{E} = E\,(\cos\delta + \mathrm{j}\,\sin\delta)$ and series impedance $\underline{Z} = R + \mathrm{j}\,X$, and a generic bus with:

- A constant power load. Active and reactive power absorbed by the load, P and Q, are independent of bus voltage, $\underline{V}$, that is considered the phase origin, $\underline{V} = V$.
- An electric vehicle load with constant active power consumption, P_{EV}, and controllable reactive power, Q_{EV}.
- A renewable generator with fluctuating active power and constant reactive power generation, P_g and Q_g.

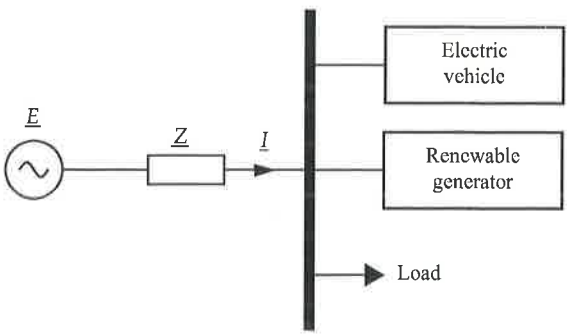

Figure 10.5 Simplified representation of a generic bus

If the current phasor flowing from the grid towards the bus, $\underline{I}$, is expressed in terms of powers:

$$\underline{I} = \left[\left(P + P_{EV} - P_g\right) - \mathrm{j}\left(Q + Q_{EV} - Q_g\right)\right]/V, \tag{10.3}$$

the bus voltage, $\underline{V} = \underline{E} - \underline{Z}\underline{I}$, can be written as

$$\begin{aligned} V = {} & E(\cos\delta + \mathrm{j}\sin\delta) - \left[R\left(P + P_{EV} - P_g\right) + X\left(Q + Q_{EV} - Q_g\right)\right]/V \\ & + \mathrm{j}\left[X\left(P + P_{EV} - P_g\right) - R\left(Q + Q_{EV} - Q_g\right)\right]/V \end{aligned} \tag{10.4}$$

As δ is small, the imaginary part of (10.4) is negligible and:

$$V^2 - EV + R\left(P + P_{EV} - P_g\right) + X\left(Q + Q_{EV} - Q_g\right) \approx 0 \tag{10.5}$$

Fluctuations of the active power generated at the bus, ΔP_g, along with possible variations of the reactive power consumed by the EV, ΔQ_{EV}, lead to bus voltage variations, ΔV. Taking into account that P, Q, P_{EV} and Q_g are supposed to be independent of voltage, and neglecting second-order terms in (10.5):

$$\Delta V \approx \left(R\Delta P_g - X\Delta Q_{EV}\right)/(2V - E) \tag{10.6}$$

In transmission grids, voltage is mostly sensitive to reactive power variations because R is small in comparison with X. In distribution grids, where R and X are similar, the bus voltage is sensitive to variations in both active and reactive powers. The first term of (10.6) shows that fluctuations of the active power injected in the bus do induce voltage fluctuations. But the second term of (10.6) shows that a controllable reactive power consumption from an EV can compensate these fluctuations.

10.3.2 Unbalanced three-phase power flow

Equation (10.6) gives a first approach to the problem in balanced grids and it is helpful for understanding the general idea. However, it is not suitable for a quantitative assessment in real distribution networks, with unbalanced loads, asymmetry of untransposed lines, and single-phase lines. In this case, more sophisticated analysis tools, like an unbalanced three-phase load flow, are needed [22]. For example, [23] describes a formulation based on current residuals in the sequence frameware, for a N bus network with N_g PV buses (buses in which active power and voltage are specified), the $6N$ unknowns are the real and imaginary parts of zero (0), positive (1) and negative (2) sequence bus voltages. The corresponding $6N$ current mismatch equations can be written as

$$\begin{aligned} \Delta\underline{I}_i^{(j)} &= \underline{I}_{ls,i}^{(j)} + \sum_{k=1}^{N}\sum_{m=0}^{2}\left[\underline{Y}_{ik}^{(j,m)}\underline{V}_k^{(m)}\right], \quad \text{with } i,k \\ &= 1,2,\ldots N;\ j,\ m = 0,1,2 \end{aligned} \tag{10.7}$$

where: j, m are the indices for sequence components; i, k are the subscripts for buses i and k, respectively; $\underline{I}_{ls,i}^{(j)}$ is the current demanded at bus i for sequence j due to the loads and generators connected to the bus; $\underline{V}_k^{(m)} = V_{r,k}^{(m)} + \mathrm{j}\, V_{x,k}^{(m)}$ represents the complex voltage at bus k and sequence component m and $\underline{Y}_{ik}^{(jm)} = G_{ik}^{(j,m)} + \mathrm{j}B_{ik}^{(j,m)}$ is the sequence component admittance matrix element that connects bus i with bus k.

The system of $6N$ nonlinear complex equations (10.7) can be solved by a Newton-Raphson recursive algorithm by splitting it into $12N$ nonlinear real equations for the real and imaginary parts of current mismatches:

$$\Delta I_{r,i}^{(j)} = I_{lsr,i}^{(j)} + \sum_{k=1}^{N} \sum_{m=0}^{2} \left[G_{ik}^{(j,m)} V_{r,k}^{(m)} - B_{ik}^{(j,m)} V_{x,k}^{(m)} \right] \tag{10.8}$$

$$\Delta I_{x,i}^{(j)} = I_{lsx,i}^{(j)} + \sum_{k=1}^{N} \sum_{m=0}^{2} \left[B_{ik}^{(j,m)} V_{r,k}^{(m)} + G_{ik}^{(j,m)} V_{x,k}^{(m)} \right] \tag{10.9}$$

10.3.3 Contribution of electric vehicles to voltage control

While an EV is connected to the grid through a power electronic converter for recharging, or even for injecting power into the grid in case of a bidirectional converter, the main function of the grid-side part of the converter is to keep the voltage of its DC link constant by transferring the active power from the grid to the vehicle, or vice versa. But advanced converters are also able to interchange reactive power with the grid, within given limits that are defined by a current, I_{max}, or a volt-ampere (VA) constraint, S_{max}, sometimes complemented with other limits related to stability or other practical issues. According to (10.6), for a balanced system and for a given active power generation ($\Delta P_g = 0$), if the converter is set to increase its reactive power consumption or decrease its reactive power injection ($\Delta Q_{EV} > 0$), the bus voltage will drop. Conversely, if a decrease in the reactive power absorption of the converter, or an injection increase, is imposed ($\Delta Q_{EV} < 0$), the bus voltage will rise. Thus, the reactive capabilities of the converter can be used for the additional objective of controlling the bus voltage.

Real power systems, particularly at the distribution level, are more complicated, as they are unbalanced, that is, the bus voltages are different for each phase. Additionally, the grid-side part of an electric vehicle power converter can adopt different topologies. A common one is a three-phase inverter, only able to interchange three-phase balanced reactive power with the grid, from just one control variable, for example, the mean of the rms voltage in each phase of a bus, as in [18]. As the electrical dynamics is much faster than that of the oscillations induced by the active power variations of renewable generators, the distribution grid can be seen as quasi-static, and the voltage phasors in each bus and phase can be computed in steady state as the response to a given time-variable input, $P_g(t)$.

10.3.4 Case study

The three-phase power flow formulation described in Section 10.3.2 allows assessing in detail the impact on the voltages at different buses on the grid of a fluctuating active power injection, $P_g(t)$, at a given bus. To illustrate its application, let us consider the European LV distribution network with DG [21] shown in Figure 10.6. This distribution grid is unbalanced due to line asymmetries and the unbalanced characteristic of the loads. In this case, the loads are modelled as constant power,

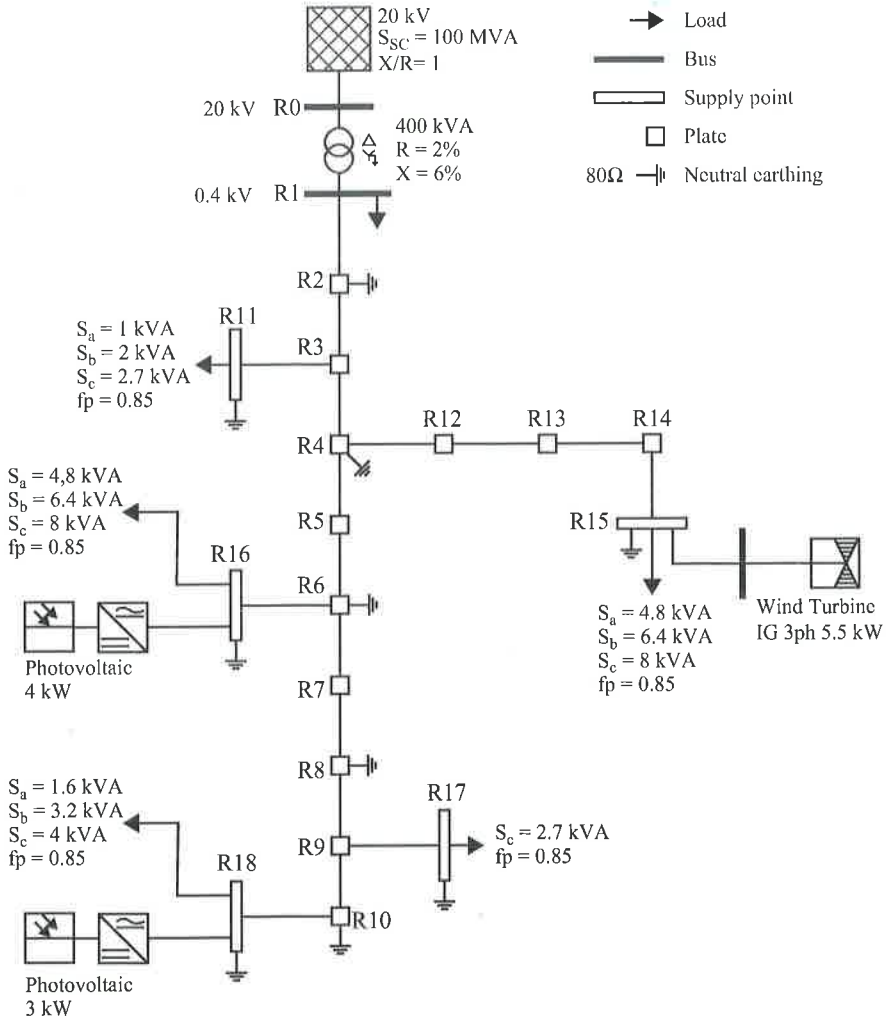

Figure 10.6 Modified European LV distribution network with distributed generation [21]

although they could be replaced by constant impedance or constant current or a combination of any of these three models.

As a case study, the original test grid is modified so as to include three EVs as part of the loads in buses R15, R16 and R18. They are modelled as constant PQ balanced loads (balanced loads in which active and reactive powers are specified) and, once connected to the grid, they absorb a constant active power of 7 kW and can absorb or generate reactive power with a limit of 5 kvar.

Figure 10.7 shows the details of each phase voltage at every bus of the modified test grid, computed by using the load-flow formulation of Section 10.3.2, without DG and electric vehicles.

To show the impact of a fluctuating active power injection from the DG at buses R15, R16 and R18, the profiles of $P_g(t)$ shown in Figure 10.8 have been considered. The active power time series from the generator at bus R15 has been obtained from the per unit profile of the base case of Figure 10.13 in [24], scaled to a rated power of 5.5 kW. Similarly, the active power time series from both PV generators, at buses R16 and R18, have been obtained from [25] and scaled to their rated power of 4 and 3 kW, respectively.

Time evolution of the grid magnitudes can be computed as successive quasi-steady states, obtained from the power flow formulation of Section 10.3.2, via a continuation load flow [26]. The black solid lines of Figure 10.9 show the thus computed time evolution of the three-phase voltages at buses R15, R16 and R18, revealing the variations induced by the fluctuating active power injection from the wind generator. Although the voltage variations are stronger at bus R15, they are also propagated to the other buses of the grid.

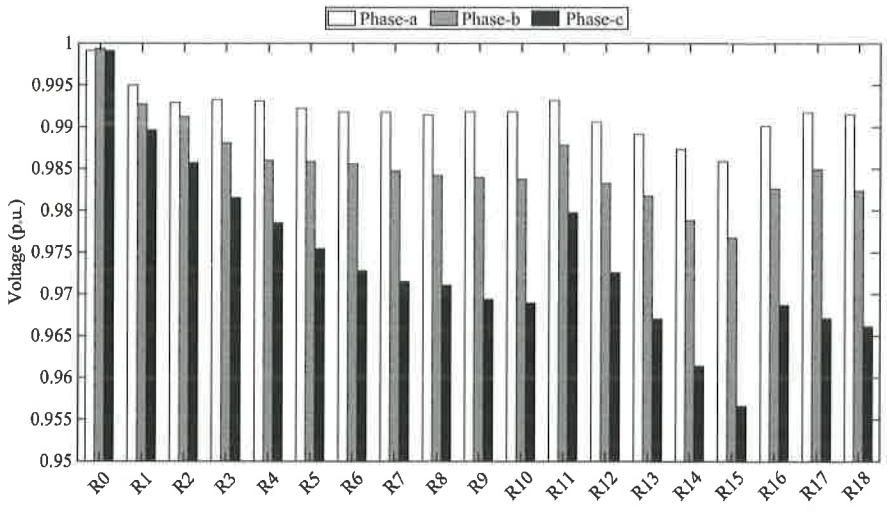

Figure 10.7 Phase voltages of the modified test network

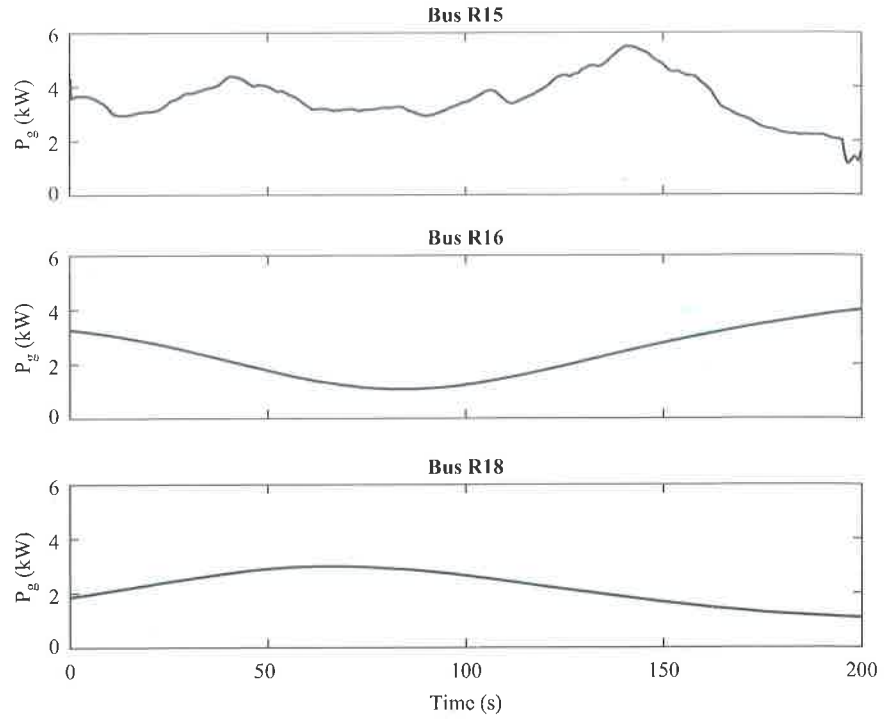

Figure 10.8 Active power injected by the distributed generation at buses R15, R16 and R18

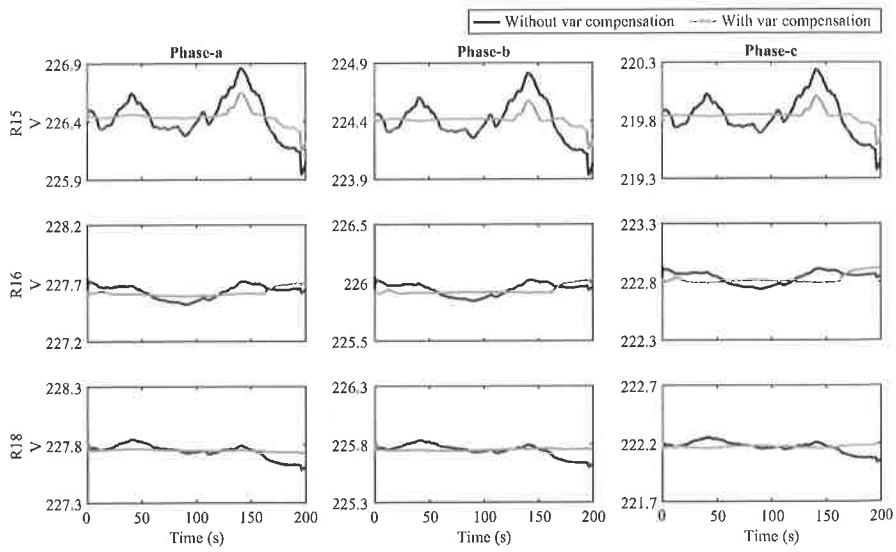

Figure 10.9 Voltage variations at buses R15, R16 and R18 induced by a fluctuating active power injection at bus R15

As stated in Section 10.3.3, the EVs connected for recharging can be used for mitigating the grid voltage fluctuations by using the reactive capability of their charger converter. For example, Figure 10.10 shows a simple implementation of a reactive power controller at a generic bus, i, where the plant is the power flow formulation of Section 10.3.2 and the outputs are the three-phase rms voltages. As the bus voltages are different for each phase and the grid-side converter is only able to generate three-phase balanced reactive power, the controller uses the mean bus voltage, defined as the mean of the rms voltage in each phase.

The grey lines of Figure 10.9 show the computed time evolution of the three-phase voltages at buses R15, R16 and R18 when the var compensation from the EVs is implemented. Generally, the voltage fluctuations are clearly smoothed.

Note, however, that there are some periods in which the reactive capability limits of the EV converters (±5 kvar) are reached and, thus, the smoothing capability is also limited. To gain a deeper insight into this issue, Figure 10.11 shows the evolution at buses R15, R16 and R18 of: the mean voltage (black solid lines), the mean voltage set point of the controller (black dotted lines) and the reactive power absorbed by the electric vehicle converters (grey solid lines).

Figure 10.12 shows the effect of using the reactive power compensation from the EVs in all the buses of the grid as the difference between the maximum and minimum voltages of the period at each phase.

A more systematic analysis of the reduction of voltage fluctuations can be derived by extending the [27] definition for balanced networks to an unbalanced power system as

$$VF_{k\Phi} = 1/T \sum_{t=1}^{T} |V_{k\Phi}(t) - V_{k\Phi}(t-1)| \tag{10.10}$$

where T is the number of time samples of the period under study and $VF_{k\Phi}$ is the voltage fluctuation index at bus k and phase Φ. From this, the system average

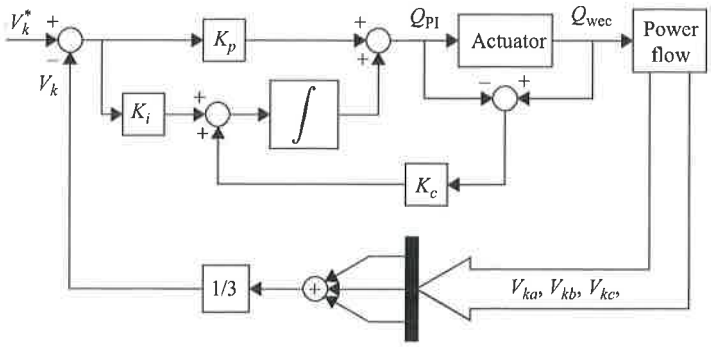

Figure 10.10 Simple reactive power controller for the electric vehicle grid-side converter

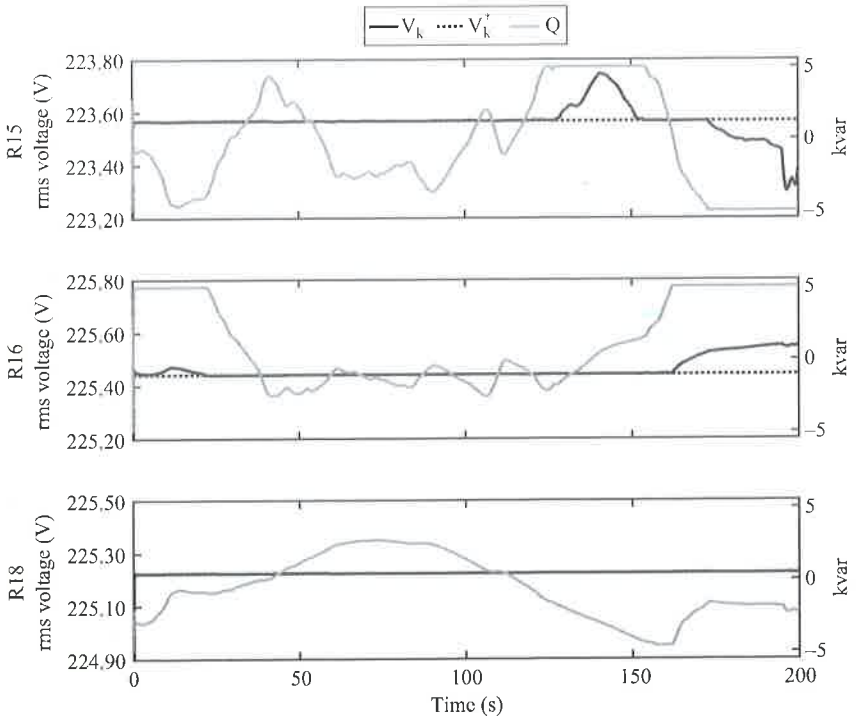

Figure 10.11 Evolution of voltage and reactive power

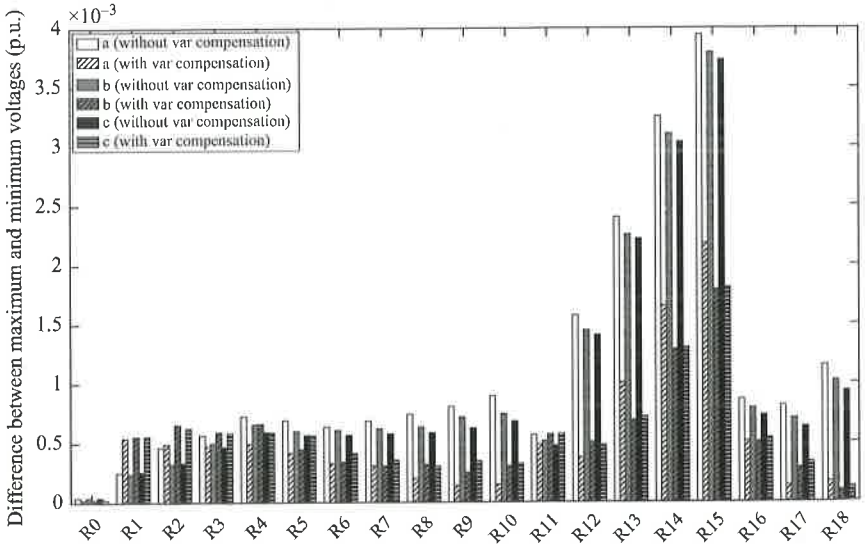

Figure 10.12 Difference between maximum and minimum voltage per bus and phase, without and with reactive compensation from electric vehicles

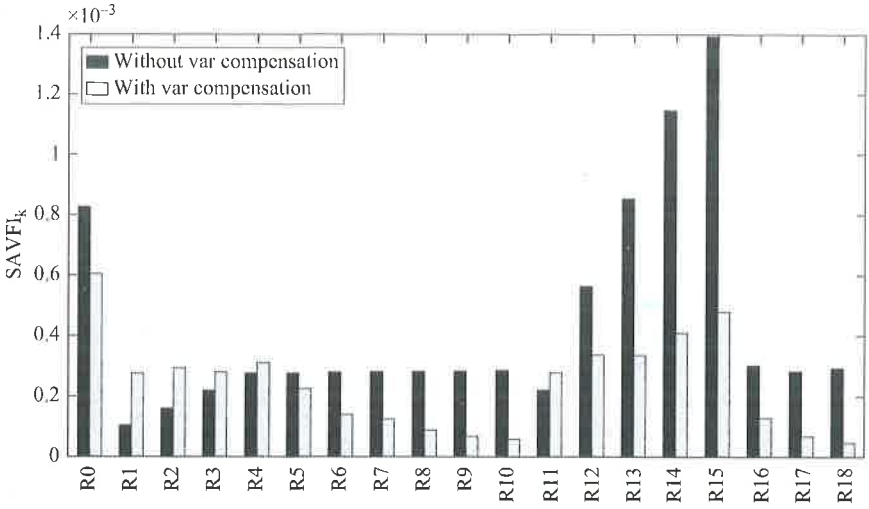

Figure 10.13 System average voltage fluctuation index per bus, with and without reactive power compensation from electric vehicles

voltage fluctuation index (SAVFI) per bus [28] can be computed as

$$\mathrm{SAVFI}_k = 1/n_\Phi \sum\nolimits_{\Phi\epsilon} \kappa VF_{k\Phi} \tag{10.11}$$

where n_Φ and κ are the number and set of phases at bus k, respectively. Figure 10.13 shows the SAVFI for each bus of the test network for the 200 s period under consideration, without and with reactive power compensation.

10.4 Conclusion

This chapter has shown how EVs connected to a power system for recharging can be used as providers of the ancillary services of primary frequency control, inertia and voltage control. Appropriate control strategies have been presented for these services and their effectivity has been tested for some simulation case studies. Further research will include a wider variety of cases and practical implementation at a microgrid.

Acknowledgements

This work was supported in part by the European Commission under project OPS Master Plan for Spanish Ports (grant number: 2015-EU-TM-0417-S) that is co-financed by the Connecting Europe Facility (CEF) for the building of the European Union's TEN-T. It was also supported in part by the Secretaria de Educacion Superior, Ciencia,

Tecnologia e Innovacion (SENESCYT), Government of the Republic of Ecuador (grant number: 2015-AR6C5141). The authors would also like to thank the companies ELECGALAPAGOS S.A. and EOLICSA for providing information related to the wind-diesel power system of the San Cristobal Island (Galapagos, Ecuador).

References

[1] International Renewable Energy Agency, Renewable Power Generation Costs in 2017, Jan. 2018.

[2] Yong, J. Y., Ramachandaramurthy, V. K., Tan, K. M., and Mithulananthan, N. A. 'Review on the state-of-the-art technologies of electric vehicle, its impacts and prospects', Renewable and Sustainable Energy Reviews, vol. 49, pp. 365–385, 2015.

[3] Fernandez, L., Roman, T., Cossent, R., Domingo, C. M., and Frias, P. 'Assessment of the impact of plug-in electric vehicles on distribution networks', IEEE Transactions on Power Systems, vol. 26, no. 1, pp. 206–213, 2011.

[4] Kempton, K., and Tomic, J. 'Vehicle-to-grid power implementation: From stabilizing the grid to supporting large-scale renewable energy', Journal of Power Sources, vol. 144, no. 1, pp. 280–294, 2005.

[5] Andersen, P. B., Marinelli, M., Olesen, O. J., *et al.* 'The Nikola project intelligent electric vehicle integration', In IEEE PES Innovative Smart Grid Technologies, Europe, Istanbul, pp. 1–6, 2014.

[6] Knezovic, K., Martinenas, S., Andersen, P. B., Zecchino, A., Marinelli, M. 'Enhancing the role of electric vehicles in the power grid: Field validation of multiple ancillary services', IEEE Transactions on Transportation Electrification, vol. 3, no. 1, pp. 201–209, 2017.

[7] Galus, M. D., Koch, S., and Andersson, G. 'Provision of load frequency control by PHEVs controllable loads and a cogeneration unit', IEEE Transactions on Industrial Electronics, vol. 58, no. 10, pp. 4568–4582, 2011.

[8] Masuta, T., and Yokoyama, A. 'Supplementary load frequency control by use of a number of both electric vehicles and heat pump water heaters', IEEE Transactions on Smart Grid, vol. 3, no. 3, pp. 1253–1262, 2012.

[9] Falahati, S., Taher, S. A., and Shahidehpour, M. 'Smart deregulated grid frequency control in presence of renewable energy resources by EVs charging control', IEEE Transactions on Smart Grid, vol. 9, no. 2, pp. 1073–1085, 2018.

[10] Lee, J., Muljadi, E., Srensen, P., and Kang,Y. C. 'Releasable kinetic energy-based inertial control of a DFIG wind power plant', IEEE Transactions on Sustainable Energy, vol. 7, no. 1, pp. 279–288, 2016.

[11] Barr, J., and Majumder, R. 'Integration of distributed generation in the Volt/var management system for active distribution networks', IEEE Transactions Smart Grid, vol. 6, no. 2, pp. 576–586, 2015.

[12] Wang, L., Yan, R., and Saha, T. K. 'Voltage management for large scale PV integration into weak distribution systems', IEEE Transactions on Smart Grid, vol. 9, no. 5, pp. 4128–4139, 2018.

[13] Cheng, L., Chang, Y., and Huang, R. 'Mitigating voltage problem in distribution system with distributed solar generation using electric vehicles', IEEE Transactions on Sustainable Energy, vol. 6, no. 4, pp. 1475–1484, 2015.

[14] Parchure, A., *et al.* 'Investigating PV generation induced voltage volatility for customers sharing a distribution service transformer', IEEE Transactions on Industry Applications, vol. 53, no. 1, pp. 71–79, 2017.

[15] Woyte, A., *et al.* 'Voltage fluctuations on distribution level introduced by photovoltaic systems', IEEE Transactions on Energy Conversion, vol. 21, no. 1, pp. 202–209, 2006.

[16] Tong, X., *et al.* 'DC voltage follow-up control for mitigating the power fluctuation of distributed generation', En Industrial Electronics Society, IECON 2017-43rd Annual Conference of the IEEE. IEEE, pp. 6380–6383, 2017.

[17] Shivashankar, S., *et al.* 'Mitigating methods of power fluctuation of photovoltaic (PV) sources–A review', Renewable and Sustainable Energy Reviews, vol. 59, pp. 1170–1184, 2016.

[18] Mendonça, H., de Castro, R., Martinez, S., and Montalban, D. 'Voltage impact of a wave energy converter on an unbalanced distribution grid and corrective actions', Sustainability, vol. 9, no. 10, pp. 1–16, 2017.

[19] Kundur, P. '*Power system stability and control*', 1st ed. New York: McGraw-Hill, 1994.

[20] Anderson, P. M., and Fouad, A. A. '*Power system control and stability*', 2nd ed. Piscataway, N.J.: IEEE Press, Wiley-Interscience, 2003.

[21] Strunz, K., Abbasi, E., Fletcher, R., and Joos, G. 'TF C6. 04.02: TB 575–Benchmark systems for network integration of renewables and distributed energy resources', CIGRE, Technical Report, 2014.

[22] Balamurugan, K., and Srinivasan, D. 'Review of power flow studies on distribution network with distributed generation', In Proceedings of the IEEE 2011 IEEE Ninth International Conference on Power Electronics and Drive Systems (PEDS), Singapore, 5–8, pp. 411–417, Dec. 2011.

[23] Mayordomo, J., Izzeddine, M., Martinez, S., Asensi, R., Exposito, A. G., and Xu, W. 'Compact and flexible three-phase power flow based on a full Newton formulation', IEE Proceedings on Generation, Transmission and Distribution, vol. 149, no. 2, pp. 225–232, 2002.

[24] Ochoa, D., and Martinez, S. 'Frequency dependent strategy for mitigating wind power fluctuations of a doubly-fed induction generator wind turbine based on virtual inertia control and blade pitch angle regulation', Renewable Energy, vol. 128, part A, pp. 108–124, 2018.

[25] Bureau of Metrology of the Australian Government. 'About one minute solar data', 29 August 2012. Retrieved from http://www.bom.gov.au/climate/data/oneminsolar/about-IDCJAC0022.shtml

[26] Ajjarapu, V., and Christy, C. 'The continuation power flow: A tool for steady state voltage stability analysis', IEEE Transactions in Power Systems, vol. 7, no. 1, pp. 416–423, 1992.

[27] Viawan, F. A., and Karlsson, D. 'Combined local and remote voltage and reactive power control in the presence of induction machine distributed generation', IEEE Transactions on Power Systems, vol. 22, no. 4, pp. 2003–2012, 2007.

[28] Ding, F., Nagarajan, A., Baggu, M., *et al.* 'Application of autonomous smart inverter Volt-VAR function for voltage reduction energy savings and power quality in electric distribution systems: Preprint', Technical Report, National Renewable Energy Laboratory(NREL): Golden, CO, USA, 2017.